Transition metal sublattice magnetization and the anomalous Hall effect in (110)-$ErFe_2/YFe_2$ multilayers

K. N. Martin, C. Morrison, G. J. Bowden, and P. A. J. de Groot
School of Physics and Astronomy, University of Southampton, Southampton SO17 1BJ, United Kingdom

R. C. C. Ward
Clarendon Laboratory, Oxford University, Oxford OX1 3PU, United Kingdom

(Received 30 April 2008; revised manuscript received 26 September 2008; published 4 November 2008)

Bulk magnetometry and anomalous Hall effect measurements are presented and discussed, for rare earth (RE)–transition metal compound superlattices, grown by molecular beam epitaxy. The results are complemented with modeled hysteresis curves. It is found that there is good agreement between the anomalous Hall effect and the calculated Fe magnetization curve. This suggests that the anomalous Hall effect, in the $REFe_2$ intermetallics, is driven predominantly by the magnetization M_{Fe} of the transition metal sublattice, and not by the total magnetization M. In addition, it is shown that the anomalous Hall effect in the superlattice (110)-[$ErFe_2$(50 Å)/YFe_2(150 Å)]×23 can be used to follow the complicated magnetization reversal processes found at high temperatures.

DOI: 10.1103/PhysRevB.78.172401 PACS number(s): 72.15.Gd, 75.70.Cn, 75.60.Jk

Since its discovery in 1881 (Refs. 1 and 2) the ordinary Hall effect (OHE) has been a well studied and highly useful phenomenon. By way of contrast, the anomalous Hall effect (AHE) is still poorly understood, over a century since its discovery. In recent years, however, there has been renewed interest in the AHE, due partly to potential applications in field sensors and memory devices,[3] and its usefulness in characterizing thin films with a perpendicular component of magnetization.[4] The effect has proved particularly useful for studying double layered perpendicular magnetic recording media,[5,6] allowing the magnetization processes of the storage layer and soft underlayer to be studied independently. In general, the Hall resistivity ρ_{xy} takes the form $\rho_{xy}=\mu_0(R_0H+R_sM)$.[7–10] Here the first term represents the ordinary Hall effect, driven by the applied field B and characterized by the ordinary Hall coefficient R_0. The second term is the anomalous component, characterized by the spontaneous Hall coefficient R_s and driven by the perpendicular magnetization M. There are several different models of the AHE (see below); however, it is generally accepted that the effect is due to the spin-orbit coupling associated with the conduction electrons, close to the Fermi surface.[10]

Research into exchange spring magnets has flourished in recent years.[11–17] Early work focused on potential applications in permanent magnets.[13,14] But more recently, exchange spring media have been proposed for magnetic data storage and microelectromechanical systems (MEMS).[18–20] Epitaxial RE-Fe superlattices (RE is a heavy rare earth), grown by molecular beam epitaxy (MBE), have proved to be ideal model systems in which to study exchange spring phenomena.[11,21] In these multilayers, magnetic exchange springs are set up in the soft YFe_2 layers. They display properties such as tunable coercivity,[22] exchange spring-driven giant magnetoresistance (GMR),[23] and spin-flop transitions.[24,25]

The spin configurations in $ErFe_2/YFe_2$ multilayers were previously studied by Martin *et al.*[24,25] using bulk magnetometry and micromagnetic modeling. Magnetic data were obtained with a vibrating-sample magnetometer (VSM), using applied fields B_{app} of up to 12 T, within a temperature range of 10–310 K.[26] Micromagnetic one-dimensional (1D) simulations were performed using the finite difference method with the object-oriented micromagnetic framework (OOMMF) software.[27] The qualitative agreement between experiment and simulation is very good. These results showed a surprising temperature dependence of the magnetic reversal of these multilayers. At sufficiently high fields, applied perpendicular to the multilayer film plane, the energy is minimized by an exchange spring-driven multilayer spin flop. In this state, the average magnetization of the $ErFe_2$ layers switches into a nominally hard in-plane axis, perpendicular to the applied field.

In this Brief Report, bulk magnetometry and Hall effect measurements on Laves phase $ErFe_2/YFe_2$ multilayers are reported and discussed. $ErFe_2/YFe_2$ superlattices are characterized by strong (~600 K) Fe-Fe ferromagnetic exchange, plus a strong antiferromagnetic (AF) Er-Fe exchange. In zero field, the superlattices can be described as man-made AF magnets with the magnetizations of the $ErFe_2$ and YFe_2 layers opposite to each other. The magnetocrystalline easy axes in the hard $ErFe_2$ layers lie parallel to a ⟨111⟩ type crystal axes, but a strain term induced by the sapphire substrate favors out-of-plane magnetization.[28] Both the magnetocrystalline anisotropy and Er magnetization fall off rapidly with temperature.[29]

The magnetization data were collected for the (110) MBE-grown multilayer [$ErFe_2$(50 Å)/YFe_2(150 Å)]×20 using a uniaxial VSM. In all cases, the applied field of up to 12 T was directed along the [110] growth direction. The magnetometry results show out-of-plane magnetization, which generates the anomalous Hall effect. The transport data were collected in-house, for the multilayer [$ErFe_2$(50 Å)/YFe_2(150 Å)]×23 using applied fields of up to 14 T. The (110)-multilayers were grown by MBE following a procedure described elsewhere.[30] The modeled hysteresis curves were calculated by numerical methods, using the

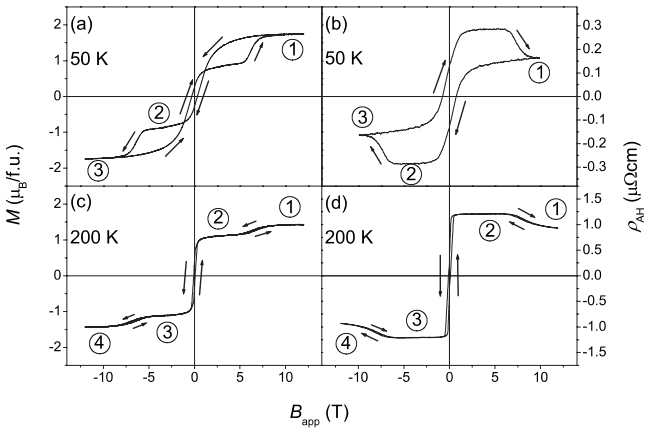

FIG. 1. Experimental results at 50 K [(a) and (b)] and 200 K [(c) and (d)]. The left-hand panels [(a) and (c)] show the magnetization and the right-hand panels [(b) and (d)] show the anomalous Hall effect. The arrows show the direction in which the field is being swept.

1–3D magnetic exchange spring model of Bowden *et al.*,[31] the Er anisotropy parameters of Martin *et al.*,[29] and the first-order strain parameter of Bowden *et al.*[32] The results are in good accord with OOMMF calculations mentioned earlier.

Figure 1 shows the experimental data collected at 50 K [(a) and (b)] and 200 K [(c) and (d)], while Fig. 2 shows the directions of the *average* moments, around the magnetic loop. The magnetic reversal at 50 K [Fig. 1(a)] is relatively simple. At high fields [see point 1 in Figs. 1(a), 1(b), and 2(a)], the Er magnetization points out of plane near to the applied field direction. As a result, there is a tight exchange spring in the soft YFe_2 layers. All moments are confined to the $[11\bar{1}]$-[110] plane. Hereafter, we shall refer to this spin

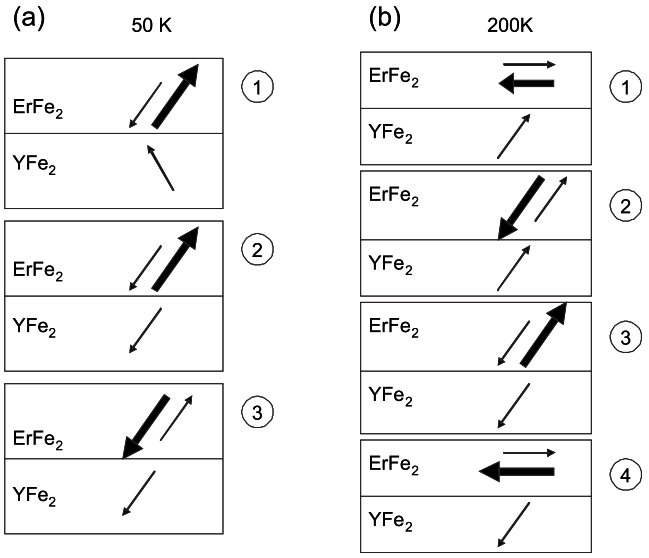

FIG. 2. Schematic representations of the spin configurations that occur during magnetic reversal at 50 K (a) and 200 K (b). The thick (thin) arrows indicate the average direction of the Er (Fe) moments, respectively. The numbers in circles correspond to the points on the experimental data (Fig. 1). At 50 K (200 K) the moments are confined to the $[11\bar{1}]$-[110] and [110]-$[\bar{1}1\bar{1}]$ planes, respectively.

configuration as the *vertical spring configuration*. On reducing the field, the exchange springs in the soft layers unwind reversibly. One consequence of this unwinding is that for multilayers with sufficiently thick YFe_2 layers, the magnetization reverses before the applied field reaches zero. This occurs for $[ErFe_2(50\ \text{Å})/YFe_2(150\ \text{Å})]\times 20$, as shown in Figs. 1(a) and 1(b). Thus the conventionally defined coercivity of this multilayer is negative, a familiar feature of exchange spring multilayers with relatively thick soft layers.[33] For this multilayer at 50 K, the measured coercivity B_C is −0.30(3) T. On reducing the field to zero, the exchange spring unwinds completely, and the multilayer enters an AF configuration with the YFe_2 and $ErFe_2$ net magnetizations opposing each other. This corresponds to point 2 in Figs. 1(a), 1(b), and 2(a). At this point, the out-of-plane component of the Fe magnetization is a maximum, giving rise to the largest value of the AHE [Fig. 1(b)]. When the applied field reaches a sufficiently high negative value, the hard $ErFe_2$ layer switches irreversibly to point close to the now negative field direction. Now the magnetic moments are in the reverse *vertical spring configuration*. This corresponds to point 3 in Figs. 1(a), 1(b), and 2(a). The field required to switch the hard layers at 50 K is 5.5(2) T. After the switch, the hard Er moments point roughly in the direction of the applied field. This is accompanied by the formation of a tight exchange spring in the YFe_2 layer, leading to an increase in overall magnetization, but a diminution in the magnitude of the overall Fe moment and hence the AHE. At low temperatures, the magnetic reversal of the multilayer is relatively simple. In summary, the moments never leave the $[11\bar{1}]$-[110] plane, and the magnetic loop is characterized by just one irreversible transition at high fields.

At 200 K [Figs. 1(c), 1(d), and 2(b)] the magnetic reversal process is more complicated, involving more than one irreversible switch. At high fields (point 1), the average $ErFe_2$ magnetization lies almost perpendicular to the applied field, close to one of the in-plane ⟨111⟩ axes, e.g., the $[\bar{1}1\bar{1}]$ axis. Concomitantly, there is a tight exchange spring in the soft YFe_2 layers. For our purposes, we shall refer to this spin arrangement as the *spin-flop configuration*. Here the Er moments take advantage of one of the four in-plane magnetocrystalline local minima. Note that all the moments are confined, primarily, to the $[\bar{1}1\bar{1}]$-[110] plane (cf. the $[11\bar{1}]$-[110] plane at low temperatures). However, as the field is decreased below about 6 T the average $ErFe_2$ magnetization rotates both *downward and sideways* to the $[\bar{1}\bar{1}\bar{1}]$-$[\bar{1}\bar{1}0]$ plane, roughly opposite to the applied field. This irreversible rotation causes the first step in the hysteresis loop. At this point (2) the multilayer reverts to a *vertical spring configuration*. However, this spin configuration differs from the low-temperature version in that the Fe moments are now more dominant. The Fe moments are aligned with the applied field, generating a large AHE [Fig. 1(d)]. Further, upon reducing the field to −0.4(1) T, the $ErFe_2$ layers switch again, pointing out of plane nearly opposite the applied field direction, but still in the $[\bar{1}\bar{1}0]$-$[\bar{1}\bar{1}\bar{1}]$ plane. This constitutes the second irreversible step, which can be described simply as simple switching of the soft YFe_2 magnetization. The multilayer is now in the reverse *vertical spring configura-*

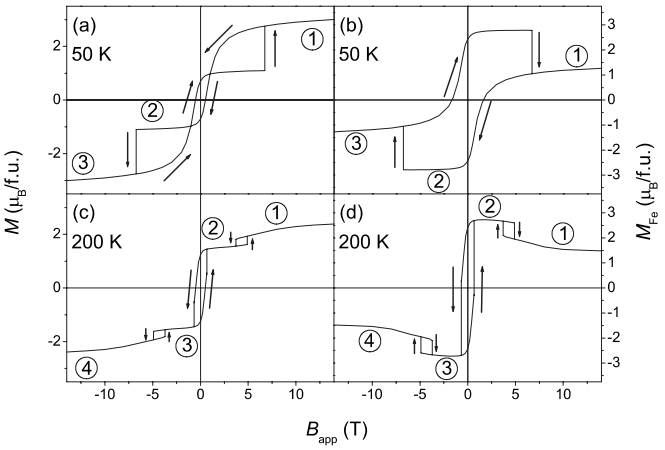

FIG. 3. Calculated results at [(a) and (b)] 50 K and [(c) and (d)] 200 K. The left-hand panels [(a) and (c)] show the full magnetization curve and the right-hand panels [(b) and (d)] show the component of the magnetization due to the Fe alone. The arrows show the direction in which the field is being swept.

tion, i.e., with the moments in the opposite direction. This too generates a large AHE, but with the opposite sign to that at point 2. Finally, when the field is reduced to below −8 T (point 4), the Er magnetization rotates to take advantage of an in-plane ⟨111⟩ axis taking up the *reverse spin-flop configuration*. This spin configuration has less Fe aligned along the field direction and so gives rise to a smaller AHE signal.

Figure 3 shows calculated hysteresis curves for 50 K [(a) and (b)] and 200 K [(c) and (d)]. The left-hand panels of Figs. 3(a) and 3(c) show the total magnetization of the multilayer, whereas the right-hand panels of Figs. 3(b) and 3(d) show the calculated Fe magnetization. It will be seen that there is a high degree of correlation between the AHE and the Fe magnetization curve at both (b) 50 K and (d) 200 K. Further, the agreement between the experimental and modeled magnetization data is very good.

This strongly suggests that the anomalous Hall effect is described by $\rho_{xy}=\mu_0(R_0H+R_sM_{\mathrm{Fe}})$ and not by the generally accepted formula $\rho_{xy}=\mu_0(R_0H+R_sM)$,[10] at least in the $ErFe_2/YFe_2$ multilayer considered here. Support for this point of view can be gathered from the early measurements on (i) amorphous Gd-Co (Ref. 34) and (ii) sputtered films of $Gd_{28}Fe_{72}$, $Dy_{21}Fe_{79}$, and $Tb_{21}Fe_{79}$.[35] Here, both sets of authors ascribe the AHE predominantly to the transition metal (TM) sublattice. In addition, the AHE measurements on sputtered $Gd_{17}Co_{83}$ (Ref. 36) should also be noted. This material possesses a magnetic compensation effect at ~100 K, where the AHE switches sign rapidly from −2 to +2 $\mu\Omega$ cm. In addition, the AHE shows little change in magnitude over the temperature range of 0–300 K, despite substantial changes in the total magnetization (see also Fig. 15.13 of Ref. 10). Thus it is hard to escape the conclusion that the AHE effect is generated by the Co sublattice alone. By way of contrast, measurements on the ternary alloys Co-Gd-Mo and Co-Gd-Au,[37] and more recently on Tb_xCo_{1-x} sputtered films,[38] have been interpreted in terms of contributions from both the Tb and Co sublattices.

Given the current disagreement in the literature, it is useful to consider what can be gleaned from theory. Band-structure calculations for the heavy $REFe_2$ series were carried out by Brooks *et al.*[39] and by Saini *et al.*[40] for $GdFe_2$. The former have shown that in addition to localized 4*f* RE moments, the $REFe_2$ compounds are characterized by 5*d* moments at the RE sites. But the 5*d* moments are driven primarily by the polarized 3*d* electrons associated with the Fe sublattice. In addition, the occupied 4*f* RE levels are found to be located well below the Fermi surface (−7.5 eV below ε_F; see Fig. 1 of Ref. 40) and, thus, play little role in conduction. In summary, therefore, the conduction electrons at the Fermi surface are essentially hybridized (3*d*, 4*s*) plus (5*d*, 6*s*) electrons, with the Fe sublattice dominant in driving both the 3*d* and 5*d* magnetic moments. These calculations are in fair agreement with measurements of the optical and magneto-optical properties of $GdFe_2$.[40] So given that most authors agree that the AHE effect is driven primarily by spin-orbit scattering of conduction electrons close to the Fermi surface,[10,41,42] it is not surprising to find that the AHE effect is dominated by Fe sublattice, with the localized RE 4*f* moments playing little or no role.

It should also be mentioned that a full band-structure calculation of the $ErFe_2/YFe_2$ multilayer, say, following the work of Yao *et al.*[41] (2004) on elemental Fe, will be nontrivial. First, two elements are now involved: Er and Fe. Second, the size of the unit cell must be increased to reflect the periodicity of the man-made ferrimagnetic samples. Third, in the presence of magnetic exchange springs, the Fe magnetization in the YFe_2 layers will be nonuniform. Consequently, the Berry curvature calculations of Yao *et al.* (2004), which treat the AHE in elemental Fe as an *intrinsic* spin-orbit mechanism, will have to be substantially modified to take the above features into account. But in passing, we note that the presence of field-adjustable exchange springs in the soft YFe_2 layer does provide us with a real signature that the AHE is generated predominantly by the Fe sublattice. In high magnetic fields, both the AHE and Fe magnetization decrease with increasing field, while the total magnetic moment increases, as expected. Thus the AHE cannot be described in terms of $\rho_{xy}=\mu_0(R_0H+R_sM)$.

Finally we note that there are other theoretical treatments of the AHE invoking *extrinsic* mechanisms such as (i) skew scattering and (ii) side-step mechanism, induced by impurities.[43] In this regard, we note that although the MBE samples are single crystal in nature, they possess many defects. It is simply not possible to grow films with better than 2% stoichemistry.[44] Thus the potential for impurity scattering is high.

In summary, AHE and magnetization data have been presented and discussed for YFe_2-dominated (110) MBE-grown $ErFe_2/YFe_2$ multilayers. The above results show that AHE measurements can be used as a simple method for quantifying the response of both Fe and Er to an applied field. The experimental data have been compared with model calculations of both the bulk and Fe sublattice magnetizations. The qualitative agreement between theory and experiment is good. In particular, the results show that the AHE closely follows the Fe sublattice magnetization. Thus the AHE offers a convenient and simple method for the characterization of the magnetization processes in magnetic superlattices. In par-

ticular, it has been demonstrated that the AHE results at high temperatures (200 K) mirror the complex magnetic reversal mechanisms associated with transitions between *vertical* and *spin-flop spring configurations*. Finally, we note that similar complex high-temperature magnetic-field behavior has been witnessed in $DyFe_2/YFe_2$ superlattices, using element-specific x-ray magnetic circular dichroism (XMCD).[45] However, AHE measurements can be performed at a fraction of the cost for comparative XMCD studies at a synchrotron facility.

[1] E. H. Hall, Philos. Mag. **10**, 301 (1880).
[2] E. H. Hall, Philos. Mag. **12**, 157 (1881).
[3] A. Gerber, A. Milner, M. Karpovski, B. Lemke, H. -U. Habermeir, J. Tuaillon-Combes, M. Négrier, O. Boisron, P. Mélinon, and A. Perez, J. Magn. Magn. Mater. **242-245**, 90 (2002).
[4] S. Nakagawa, A. Sato, I. Sasaki, and M. Naoe, J. Appl. Phys. **87**, 5705 (2000).
[5] S. Nakagawa, I. Sasaki, and M. Naoe, J. Appl. Phys. **91**, 8354 (2002).
[6] J. Lindemuth and B. Dodrill, IEEE Trans. Magn. **40**, 2191 (2004).
[7] C. M. Hurd, *The Hall Effect in Metals and Alloys* (Plenum, New York, 1972).
[8] A. W. Smith and R. W. Sears, Phys. Rev. **34**, 1466 (1929).
[9] E. M. Pugh, Phys. Rev. **36**, 1503 (1930).
[10] R. C. O'Handley, *Modern Magnetic Materials: Principles and Applications* (Wiley, New York, 2000).
[11] E. E. Fullerton, J. S. Jiang, and S. D. Bader, J. Magn. Magn. Mater. **200**, 392 (1999).
[12] E. E. Fullerton, J. S. Jiang, M. Grimsditch, C. H. Sowers, and S. D. Bader, Phys. Rev. B **58**, 12193 (1998).
[13] R. Skomski and J. M. D. Coey, IEEE Trans. Magn. **29**, 2860 (1993).
[14] R. Skomski and J. M. D. Coey, Phys. Rev. B **48**, 15812 (1993).
[15] D. Suess, T. Schrefl, R. Dittrich, M. Kirschner, F. Dorfbauer, G. Hrkac, and J. Fidler, J. Magn. Magn. Mater. **290**, 551 (2005).
[16] D. Suess, T. Schrefl, S. Fähler, M. Kirschner, G. Hrkac, F. Dorfbauer, and J. Fidler, Appl. Phys. Lett. **87**, 012504 (2005).
[17] R. H. Victora and X. Shen, IEEE Trans. Magn. **41**, 537 (2005).
[18] M. R. J. Gibbs, J. Magn. Magn. Mater. **290-291**, 1298 (2005).
[19] A. Ludwig and E. Quandt, J. Appl. Phys. **87**, 4691 (2000).
[20] C. T. Pan and S. C. Shen, J. Magn. Magn. Mater. **285**, 422 (2005).
[21] K. Dumesnil, M. Dutheil, C. Dufour, and P. Mangin, Phys. Rev. B **62**, 1136 (2000).
[22] M. Sawicki, G. J. Bowden, P. A. J. de Groot, B. D. Rainford, J. M. L. Beaujour, R. C. C. Ward, and M. R. Wells, Appl. Phys. Lett. **77**, 573 (2000).
[23] S. N. Gordeev, J.-M. L. Beaujour, G. J. Bowden, B. D. Rainford, P. A. J. de Groot, R. C. C. Ward, M. R. Wells, and A. G. M. Jansen, Phys. Rev. Lett. **87**, 186808 (2001).
[24] K. N. Martin, K. Wang, G. J. Bowden, A. A. Zhukov, P. A. J. de Groot, J. P. Zimmermann, H. Fangohr, and R. C. C. Ward, Appl. Phys. Lett. **89**, 132511 (2006).
[25] K. N. Martin, K. Wang, G. J. Bowden, P. A. J. de Groot, J. P. Zimmermann, H. Fangohr, and R. C. C. Ward, J. Appl. Phys. **101**, 09K511 (2007).
[26] M. Sawicki, G. J. Bowden, P. A. J. de Groot, B. D. Rainford, R. C. C. Ward, and M. R. Wells, J. Appl. Phys. **87**, 6839 (2000).
[27] M. J. Donahue and D. G. Porter, *OOMMF Users Guide* (NIST, Gaithersburg, MD, 1999).
[28] A. Mougin, C. Dufour, K. Dumesnil, and P. Mangin, Phys. Rev. B **62**, 9517 (2000).
[29] K. N. Martin, P. A. J. de Groot, B. D. Rainford, K. Wang, G. J. Bowden, J. P. Zimmermann, and H. Fangohr, J. Phys.: Condens. Matter **18**, 459 (2006).
[30] M. J. Bentall, R. C. C. Ward, E. J. Grier, and M. R. Wells, J. Phys.: Condens. Matter **15**, 4493 (2003).
[31] G. J. Bowden, K. N. Martin, B. D. Rainford, and P. A. J. de Groot, J. Phys.: Condens. Matter **20**, 015209 (2008).
[32] G. J. Bowden, P. A. J. de Groot, B. D. Rainford, K. Wang, K. N. Martin, J. P. Zimmermann, and H. Fangohr, J. Phys.: Condens. Matter **18**, 5861 (2006).
[33] J.-M. L. Beaujour, S. N. Gordeev, G. J. Bowden, P. A. J. de Groot, B. D. Rainford, R. C. C. Ward, and M. R. Wells, Appl. Phys. Lett. **78**, 964 (2001).
[34] K. Okamoto, T. Shirakawa, S. Matsushita, and Y. Sakurai, IEEE Trans. Magn. **10**, 799 (1974).
[35] Y. Mimura, N. Imamura, and Y. Kushiro, J. Appl. Phys. **47**, 3371 (1976).
[36] T. Shirakawa, Y. Nakajima, S. Okamoto, S. Matsushita, and T. Sakurao, in *Magentism and Magnetic Materials*, AIP Conf. Proc. No. 34 (AIP, New York, 1976), p. 349.
[37] T. R. McGuire, R. J. Gambino, and R. C. Taylor, J. Appl. Phys. **48**, 2965 (1977).
[38] T. W. Kim and R. J. Gambino, J. Appl. Phys. **87**, 1869 (2000).
[39] M. S. S. Brooks, L. Nordstrom, and B. Johansson, J. Phys.: Condens. Matter **3**, 2357 (1991).
[40] S. M. Saini, N. Singh, T. Nautiyal, and S. Auluck, J. Phys.: Condens. Matter **19**, 176203 (2007).
[41] Y. Yao, L. Kleinman, A. H. MacDonald, J. Sinova, T. Jungwirth, D.-s. Wang, E. Wang, and Q. Niu, Phys. Rev. Lett. **92**, 037204 (2004).
[42] A. Gerber, A. Milner, A. Finkler, M. Karpovski, L. Goldsmith, J. Tuaillon-Combes, O. Boisron, P. Mélinon, and A. Perez, Phys. Rev. B **69**, 224403 (2004).
[43] L. Berger, Phys. Rev. B **2**, 4559 (1970).
[44] A. Mougin, C. Dufour, K. Dumesnil, N. Maloufi, Ph. Mangin, and G. Patrat, Phys. Rev. B **59**, 5950 (1999).
[45] K. Dumesnil, C. Dufour, P. Mangin, F. Wilhelm, and A. Rogalev, J. Appl. Phys. **95**, 6843 (2004).